Analytical solutions for the electromagnetic fields of flattened and annular Gaussian laser modes. II. Large *F*-number laser focusing

Scott M. Sepke and Donald P. Umstadter

Department of Physics and Astronomy, University of Nebraska, Lincoln, Nebraska 68588-0111

Received March 14, 2006; accepted June 2, 2006; posted June 22, 2006 (Doc. ID 68844)

A spherical Hankel function series solution for the vector components of a general flattened Gaussian laser field is derived, based on the angular spectrum of plane waves. This perturbative series is valid for spot sizes greater than ten wavelengths, creating a complete vector solution for a general flattened Gaussian laser profile for all focusing conditions when coupled to the model developed in Part I of this investigation [J. Opt. Soc. Am. B **23**, 2157 (2006)]. The focusing and propagation properties of these fields are then explored numerically. Finally, the exact solution is compared to the perturbative Hermite–Gaussian (0,0) laser mode by comparing the focal plane boundary conditions imposed in each and is found to be a separate and distinct solution under tight focusing conditions. © 2006 Optical Society of America

OCIS codes: 140.3300, 260.2110, 350.5500.

1. INTRODUCTION

In Part I of this study, the exact solution of the wave equation for a laser having an arbitrary flattened Gaussian profile was evaluated analytically by noting that all of the integrals in the formal solution are equivalent to Gegenbauer's finite integral.[1] The resulting solution was derived without approximation, but the expansion coefficients are impractical to evaluate for laser spot sizes larger than 20 wavelengths. To accommodate this, in this paper, the integrals are evaluated again for the general flattened Gaussian profile by making use of a perturbative series in the square of the laser diffraction angle $\epsilon^2 = \lambda_0^2/\pi^2 w_0^2$, where λ_0 and w_0 are the laser wavelength and waist.

The fields and their propagation are then described numerically for some sample parameters, illustrating both flattened and annular modes. A key observation follows immediately from these calculated field distributions. Longitudinal laser fields are driven by gradients in the transverse field. In a purely Gaussian beam, this gradient is only zero along a narrow line. A flattened Gaussian profile moves appreciable gradients in the primary transverse fields away from the laser axis, and the longitudinal fields of a flat-top laser pulse are, hence, zero in a finite region about the laser axis, in stark contrast to the standard Gaussian result. This has direct implications for the modeling of laser interactions.

The importance of the accuracy of the physical model of focused laser fields has been extensively illustrated theoretically and experimentally in the high-intensity laser-plasma literature.[2–12] The form of the laser beam chosen can have a significant impact on the results predicted by a model. The solutions presented herein as well as in the previous part of this work provide analytic field models for all spot sizes and allow great flexibility in reproducing the detailed structure of a laser beam profile.

The resulting series solutions bear many similarities to the standard Hermite–Gaussian (0,0) mode in the limit of a pure Gaussian, and the question naturally arises as to their equivalence. To answer this, these modes are compared directly by analyzing the boundary conditions imposed on each, and, in fact, they are shown to be distinct solutions of the Maxwell wave equation.

2. APPROXIMATE SERIES SOLUTION

From the Fourier transform derivation of the first part of this study,[1] the six laser field components were derived exactly in integral form for a flattened Gaussian focal plane profile,

$$E_x(x,y,z=0) = \sum_{N=0}^{\infty} A_N \left(\frac{r}{w_0}\right)^{2N} e^{-(r^2/w_0^2)}, \tag{1}$$

where w_0 is the nominal Gaussian $(1/e)$ waist and $r^2 = x^2 + y^2$. The resulting asymmetric electric and magnetic field components are then

$$E_x^a = \sum \int_0^1 e^{-(b^2/\epsilon^2)} e^{imk_0 z} J_0(k_0 r b) L_N\left(\frac{b^2}{\epsilon^2}\right) b\,\mathrm{d}b,$$

$$E_z^a = i \sum \partial_{\bar{x}} \int_0^1 e^{-(b^2/\epsilon^2)} \frac{e^{imk_0 z}}{m} J_0(k_0 r b) L_N\left(\frac{b^2}{\epsilon^2}\right) b\,\mathrm{d}b,$$

$$B_x^a = \sum \partial_{\bar{x}\bar{y}}^2 \int_0^1 e^{-(b^2/\epsilon^2)} \frac{e^{imk_0 z}}{m} J_0(k_0 r b) L_N\left(\frac{b^2}{\epsilon^2}\right) b\,\mathrm{d}b,$$

$$B_y^a = \sum \left[\int_0^1 e^{-(b^2/\epsilon^2)} m e^{imk_0 z} J_0(k_0 r b) L_N\left(\frac{b^2}{\epsilon^2}\right) b\,\mathrm{d}b - \partial_{\bar{x}}^2 \int_0^1 e^{-(b^2/\epsilon^2)} \frac{e^{imk_0 z}}{m} J_0(k_0 r b) L_N\left(\frac{b^2}{\epsilon^2}\right) b\,\mathrm{d}b \right],$$

$$B_z^a = i\sum \partial_{\bar{y}} \int_0^1 e^{-(b^2/\epsilon^2)} e^{imk_0 z} J_0(k_0 r b) L_N\left(\frac{b^2}{\epsilon^2}\right) b\,db\,db,$$

and $E_y \equiv 0$. In these relations, $J_n(x)$ is the nth-order Bessel function of the first kind, $\partial_{\bar{a}}(\cdot) = k_0^{-1}\partial_a(\cdot)$, and Σ denotes $2\epsilon^{-2}E_0\Sigma_{N=0}^{\infty} A_N N!$ for arbitrary complex values of A_N, allowing a large amount of flexibility in specifying the field profile. The full, symmetric solution for the fields is then obtained by repeating this process, now specifying $B_x \equiv 0$ and B_y as a flattened Gaussian and averaging the two results.

This is a formally exact solution of the Maxwell wave equation for all values of the parameters A_N and w_0. The Gegenbauer expansion used to derive the tightly focused fields, however—for both the Gaussian and the flattened Gaussian—converges slowly when $w_0 \gtrsim 10\lambda_0$, and as $w_0 \gtrsim 20\lambda_0$, the Gaussian term $\exp[(m^2-1)/\epsilon^2]$ becomes too peaked at $m=1$ to evaluate the expansion coefficients. Physically, of course, this is the result of the beam curvature going to zero as the laser fields approach the paraxial and eventually the plane-wave limit that propagates only along the forward ($\hat{\mathbf{z}}$) direction.

Thus, to compliment this tightly focused result, a corresponding loose focusing solution is derived here. This is accomplished following the model of Cicchitelli *et al.* by expanding each integral above in a perturbative series about the small parameter ϵ^2, employing the identities

$$e^{imz} = \sum_{n=0}^{\infty} \frac{1}{n!}\left(\frac{b^2}{2}\right)^n z^{n+1} h_{n-1}^{(1)}(z),$$

$$me^{imz} = i\sum_{n=0}^{\infty} \frac{1}{n!}\left(\frac{b^2}{2}\right)^n z^n [(z)h_n^{(1)}(z) - 2nh_{n-1}^{(1)}(z)],$$

$$\frac{e^{imz}}{m} = i\sum_{n=0}^{\infty} \frac{1}{n!}\left(\frac{b^2}{2}\right)^n z^{n+1} h_n^{(1)}(z),$$

where $h_n^{(1)}(x) = j_n(x) + iy_n(x)$ is the nth-order spherical Hankel function of the first kind here defined in terms of the spherical Bessel functions of the first and second kind. The resulting fully symmetric series solution for the electric field is then

$$E_x = -iE_0\sum_{N=0}^{\infty} A_N \sum_{n=0}^{\infty} \epsilon^{2n}(k_0 z)^{n+1} h_n^{(1)}(k_0 z) \sum_{m=0}^{N} \Delta_{mn}^N \partial_{\bar{y}}^2 G_{m+n}(\xi) + E_0\sum_{N=0}^{\infty} A_N \sum_{n=0}^{\infty} \epsilon^{2n}(k_0 z)^n \{[(k_0 z) - 2in]h_{n-1}^{(1)}(k_0 z) + i(k_0 z)h_n^{(1)}(k_0 z)\} \sum_{m=0}^{N} \Delta_{mn}^N G_{m+n}(\xi), \quad (2)$$

$$E_y = iE_0\sum_{N=0}^{\infty} A_N \sum_{n=0}^{\infty} \epsilon^{2n}(k_0 z)^{n+1} h_n^{(1)}(k_0 z) \sum_{m=0}^{N} \Delta_{mn}^N \partial_{\bar{x}\bar{y}}^2 G_{m+n}(\xi), \quad (3)$$

$$E_z = E_0\sum_{N=0}^{\infty} A_N \sum_{n=0}^{\infty} \epsilon^{2n}(k_0 z)^{n+1} [ih_{n-1}^{(1)}(k_0 z) - h_n^{(1)}(k_0 z)] \sum_{m=0}^{N} \Delta_{mn}^N \partial_{\bar{x}} G_{m+n}(\xi) \quad (4)$$

for $G_{m+n}(\xi) = \exp(-\xi)L_{m+n}(\xi)$ and $\xi = r^2/w_0^2$. The magnetic field is identical except, again, the roles of x and y are reversed, and the parameter Δ_{mn}^N is defined by

$$\Delta_{mn}^N \equiv (-1)^m \left[\frac{N!N!(m+n)!}{(N-m)!n!m!m!2^{n+1}}\right].$$

In the purely Gaussian limit, that is, $A_0 = 1$ and $A_{N>0} = 0$, this reduces to

$$E_x = -iE_0\sum_{n=0}^{\infty} \epsilon^{2n}\left(\frac{k_0 z}{2}\right)^{n+1} h_n^{(1)}(k_0 z)\partial_{\bar{y}}^2 G_n\left(\frac{r^2}{w_0^2}\right) + \frac{E_0}{2}\sum_{n=0}^{\infty} \epsilon^{2n}\left(\frac{k_0 z}{2}\right)^n F_x(k_0 z) G_n\left(\frac{r^2}{w_0^2}\right),$$

$$E_y = iE_0\sum_{n=0}^{\infty} \epsilon^{2n}\left(\frac{k_0 z}{2}\right)^{n+1} h_n^{(1)}(k_0 z)\partial_{\bar{x}\bar{y}}^2 G_n\left(\frac{r^2}{w_0^2}\right),$$

$$E_z = E_0\sum_{n=0}^{\infty} \epsilon^{2n}\left(\frac{k_0 z}{2}\right)^{n+1} F_z(k_0 z)\partial_{\bar{x}} G_n\left(\frac{r^2}{w_0^2}\right), \quad (5)$$

where $F_x(z) \equiv [(z-2in)h_{n-1}^{(1)}(z) + izh_n^{(1)}(z)]$ and $F_z(z) \equiv [ih_{n-1}^{(1)}(z) - h_n^{(1)}(z)]$. Thus, a symmetrized version of the Gaussian result of Cicchitelli *et al.* is recovered.[2]

For very loose focusing, $\epsilon \ll 1$, only the first term of each series is required. The leading order terms in ϵ are then

$$E_x = 2E_0 \sin(\eta)e^{-(r^2/w_0^2)}\sum_{N=0}^{\infty}\sum_{m=0}^{N} A_N \Delta_{m0}^N L_m\left(\frac{r^2}{w_0^2}\right),$$

$$E_y = \epsilon^2 E_0 \sin(\eta)e^{-(r^2/w_0^2)}\left(\frac{xy}{r^2}\right)\sum_{N=0}^{\infty}\sum_{m=0}^{N} A_N \Delta_{m0}^N \Theta_m,$$

$$E_z = 2\epsilon E_0 \cos(\eta)e^{-(r^2/w_0^2)}\left(\frac{x}{r}\right)\sum_{N=0}^{\infty}\sum_{m=0}^{N} A_N \Delta_{m0}^N \psi_m,$$

and the functions ψ_m and Θ_m are given by

$$\psi_m(r) = m\sqrt{\xi^{-1}}[L_m(\xi) - L_{m-1}(\xi)] - \sqrt{\xi}L_m(\xi),$$

$$\Theta_m(r) = \{\xi L_m(\xi) - 2m[L_m(\xi) - L_{m-1}(\xi)] + m(m-1)\xi^{-1}[L_m(\xi) - 2L_{m-1}(\xi) + L_{m-2}(\xi)]\},$$

and are dimensionless, contributing only to the flattened Gaussian terms save for $\xi L_m(\xi)$ in Θ_m, which is equal to $(r/w_0)^2$ in the lowest-order Gaussian E_y expansion, and $\sqrt{\xi}L_m(\xi)$ in ψ_m, which is equal to (r/w_0) in the lowest-order expansion of E_z.

As anticipated by the standard Hermite–Gaussian modes, the leading order of E_x is ϵ^0, while those of E_z and E_y are ϵ and ϵ^2, respectively. Also, owing to the definition

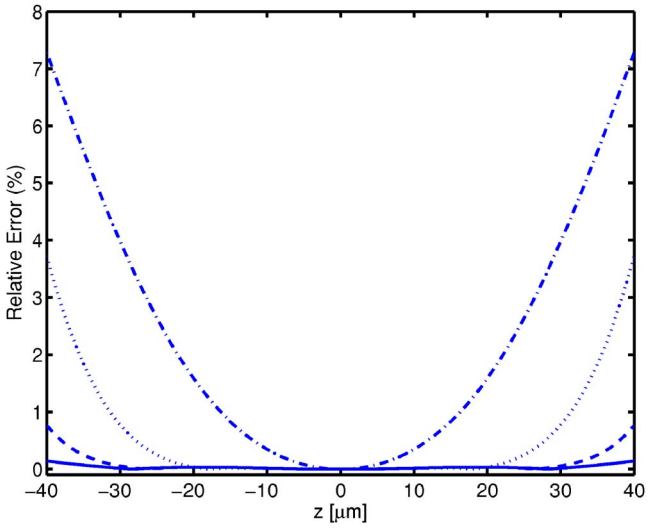

Fig. 1. (Color online) Relative error of the series expansion of E_x compared to the exact integral solution for $w_0=5$ μm along the line $(x,y)=(1,1)$ μm to the order of ϵ^0 (dotted–dashed curve), ϵ^8 (dotted curve), ϵ^{18} (dashed curve), and ϵ^{38} (solid curve) for $\lambda_0=1$ μm.

of the spherical Hankel function, each order in ϵ now shows an $\exp(i\eta)$ dependence explicitly where $\eta=k_0z-\omega_0t$ is the laser phase as in the Hermite–Gaussian modes. Thus, the question naturally arises as to the relationship between this angular spectrum of plane-wave solution and the standard perturbative paraxial–nonparaxial series. This is explored in Section 4, and, in fact, in the limit of $\epsilon^2\to 0$, the purely Gaussian mode and the Hermite–Gaussian solutions are identical, but as the laser focusing tightens, differences of the order of ϵ^2 appear.

This series expansion serves to illustrate the importance of having an exact solution. Figure 1 shows the relative error of this series expansion for E_x with a waist $w_0=5$ μm along the line $(x,y)=(1,1)$ μm for 1, 5, 10, and 20 terms of the retained series. Adding additional terms improves the approximation in the vicinity of $z=0$ and increases the range of validity, but this can become prohibitive. Then the Fourier–Gegenbauer solution becomes the practical alternative.

3. FIELD DISTRIBUTION OF FLATTENED AND ANNULAR GAUSSIAN LASERS

The formalism for each field component of pure, flattened, and annular Gaussian laser fields has now been fully developed for all focusing conditions. In this section, a more physical description is given by plotting both the focal plane distributions and the propagation characteristics of each of the field components. Even modest flattening of a beam demonstrably alters the off-polarization field distributions, and this is discussed in terms of the accuracy principle.

A. Flattened Gaussian Mode

Figure 2 shows the transverse boundary condition applied for computing the fields shown in Figs. 3–10. The constants, A_N, used in these cases are $[A_0,A_1,A_2]=[1,1,0.5]$, and all others are identically zero. The waist is $w_0=5$ λ_0 and $E_0=1$. Figures 3–5 illustrate the electric field components of the flattened Gaussian in the focal plane. As expected, E_z is of the order of ϵ and E_y of ϵ^2 relative to E_x. E_y exhibits the four lobes placed symmetrically about the origin, as in the standard Gaussian beam. Additionally, however, four smaller lobes also equally spaced around and closer to the laser axis are now present. E_z shows a significant change as well. In the purely Gaussian mode, $E_z\sim x\exp(-r^2/w^2)$, implying that this component is only identically zero in the laser polarization plane. In the flattened Gaussian case, though, an area equivalent to the flattened area in E_x is zero. This is, of course, because E_z arises from the radial gradient of E_x. This can be easily seen from Gauss's law,

$$E_z \approx -\int^z \partial_x E_x \mathrm{d}z' \sim \frac{i}{k_0}\frac{\partial E_x}{\partial x},$$

where $\epsilon\ll 1$ has been assumed for illustrative purposes. This region of zero longitudinal field is depicted more

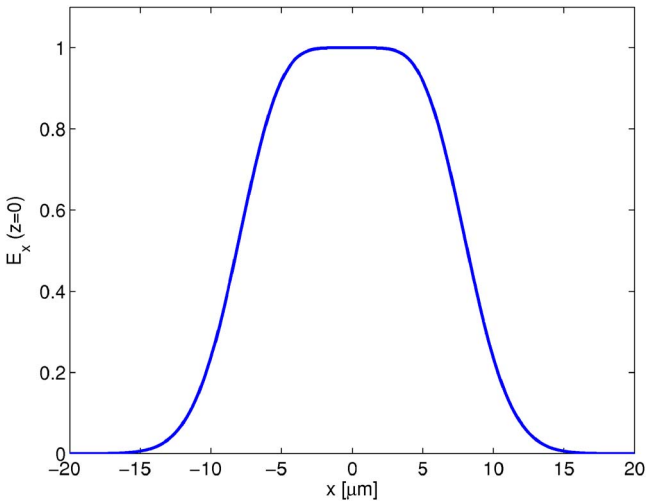

Fig. 2. (Color online) Flattened Gaussian boundary condition for a wavelength $\lambda_0=1$ μm, waist $w_0=5$ μm, $E_0=1$, and $A_N=(1,1,0.5)$.

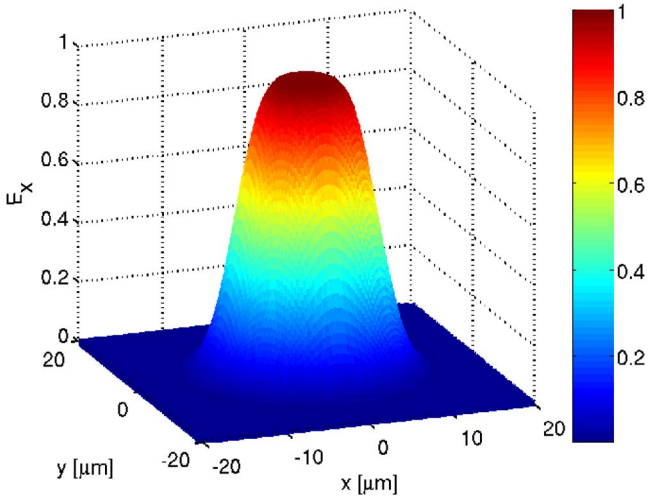

Fig. 3. (Color online) Angular spectrum solution for E_x in the focal plane $(z=0)$ for a wavelength $\lambda_0=1$ μm, waist $w_0=5$ μm, $E_0=1$, and $A_N=(1,1,0.5)$.

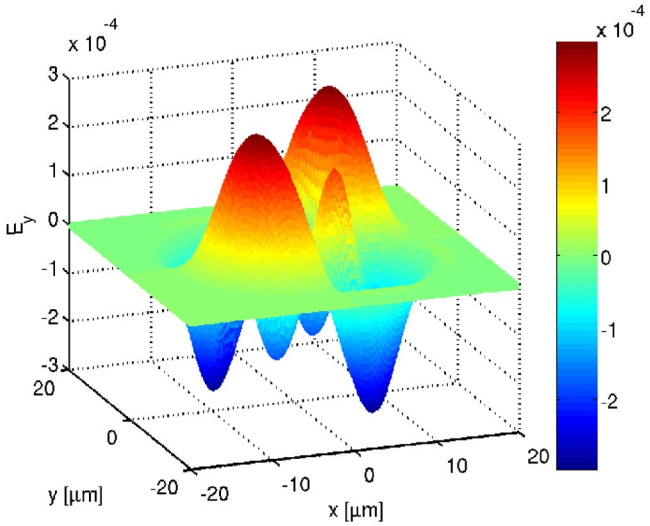

Fig. 4. (Color online) Angular spectrum solution for E_y in the focal plane ($z=0$) for a wavelength $\lambda_0=1$ μm, waist $w_0=5$ μm, $E_0=1$, and $A_N=(1,1,0.5)$.

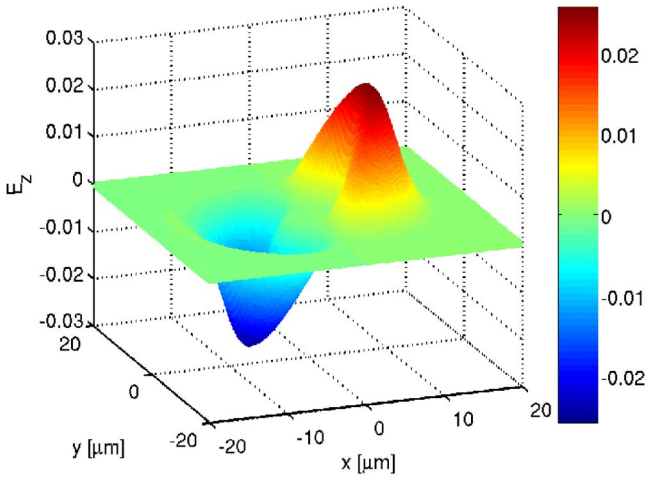

Fig. 5. (Color online) Angular spectrum solution for E_z in the focal plane ($z=0$) for a wavelength $\lambda_0=1$ μm, waist $w_0=5$ μm, $E_0=1$, and $A_N=(1,1,0.5)$.

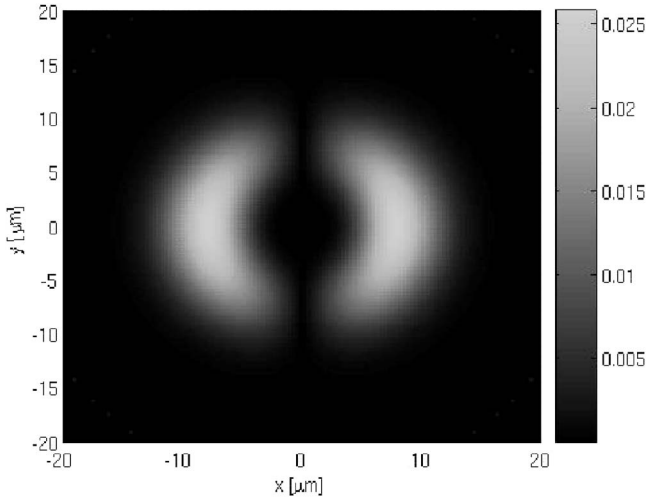

Fig. 6. Angular spectrum solution for $|E_z|$ in the focal plane ($z=0$) for a wavelength $\lambda_0=1$ μm, waist $w_0=5$ μm, $E_0=1$, and $A_N=(1,1,0.5)$. Notice the region of zero field intensity around the laser axis.

clearly in Fig. 6, which plots $|E_z|$ in the focal plane. Figure 7 shows the purely Gaussian result for comparison. Even the slight flattening of the pulse in Figs. 3–5 creates a significant deviation in the longitudinal field, which can have significant implications for relativistic electron dynamics.

Recent experiments and simulations have proven that longitudinal laser fields play a dominant role in direct laser-electron scattering when the two beams are obliquely incident.[2–12] Any deviation from a purely Gaussian profile by a given laser, either intentional or arising simply from nonidealities in the laser system, will tend to demonstrably alter the driving longitudinal fields and, hence, the laser-electron scattering characteristics.

The free-space propagation of a flattened Gaussian beam is illustrated in Figs. 8–10. The most notable feature here is that the maximum intensity now occurs away from the focal plane. The maximum value of E_x is nearly 25% larger than the focal plane value $E_0=1$ and is located

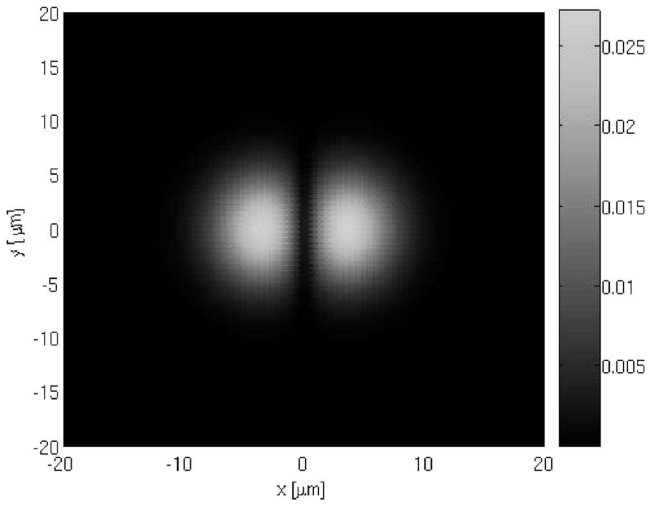

Fig. 7. Angular spectrum solution for $|E_z|$ in the focal plane ($z=0$) for a wavelength $\lambda_0=1$ μm, waist $w_0=5$ μm, $E_0=1$, and $A_N=(1)$, a pure Gaussian. Notice the region of zero field intensity around the laser axis is now only a narrow line along $x=0$.

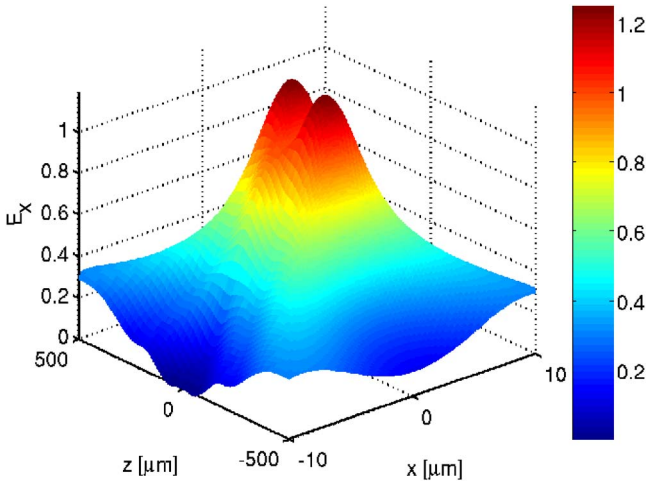

Fig. 8. (Color online) Angular spectrum solution for E_x along $x=y$ versus z for a wavelength $\lambda_0=1$ μm, waist $w_0=5$ μm, $E_0=1$, and $A_N=(1,1,0.5)$.

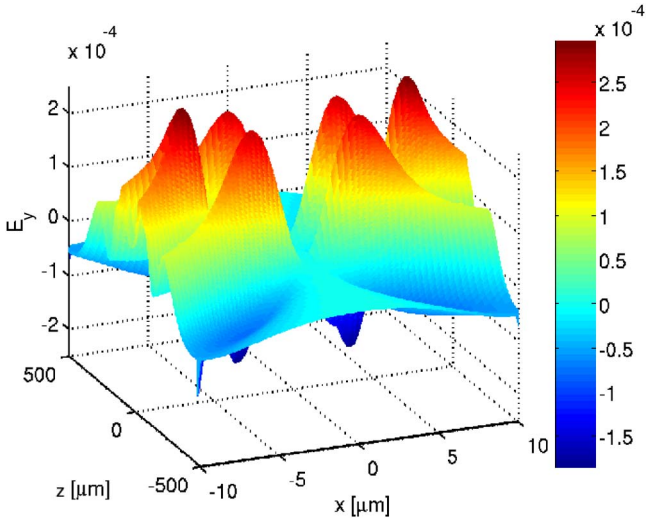

Fig. 9. (Color online) Angular spectrum solution for E_y along $x=y$ versus z for a wavelength $\lambda_0=1$ μm, waist $w_0=5$ μm, $E_0=1$, and $A_N=(1,1,0.5)$.

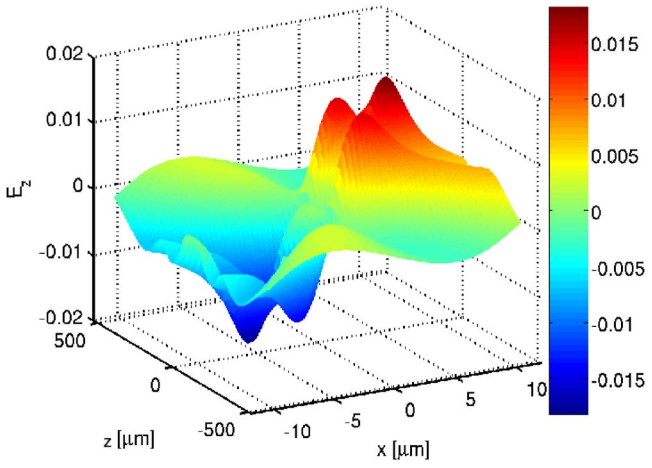

Fig. 10. (Color online) Angular spectrum solution for E_z along $x=y$ versus z for a wavelength $\lambda_0=1$ μm, waist $w_0=5$ μm, $E_0=1$, and $A_N=(1,1,0.5)$.

roughly one Rayleigh range, $z_R=k_0w_0^2/2$, along the laser axis on both sides of the focal plane. The remaining components E_y and E_z exhibit their characteristic Gaussian mode structure with the addition of the extra lobes described above.

B. Annular Gaussian Mode

The field model can also be used to model annular Gaussian laser modes by simply letting $A_0=0$. Figures 11–13 show the three electric field components in the focal plane for $A_1=1$, and all other constants equal to zero for $w_0=5$ λ_0 and $E_0=1$ as before. Again, four additional lobes are present in E_y between the purely Gaussian lobes and the laser axis. In this case, these are larger than the Gaussian contribution and are driven by the large radial gradients in E_x and E_z caused by the on-axis shadow. This gradient has also produced two dominant peaks in E_z near the axis through the same process.

Though this additional field structure in both of these laser modes has arisen from inverse processes—small

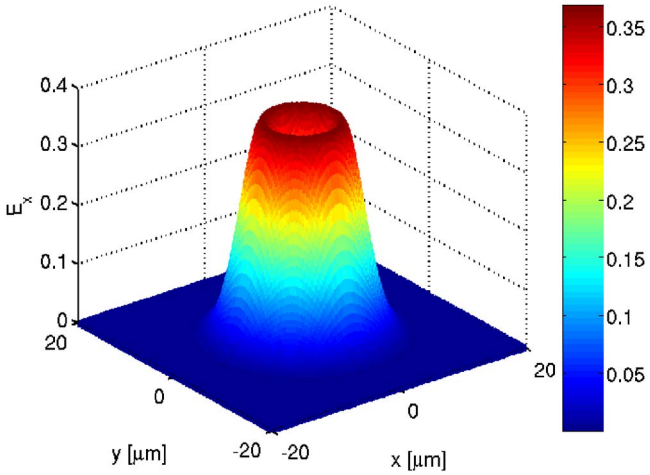

Fig. 11. (Color online) Hollow core angular spectrum solution for E_x in the focal plane ($z=0$) for a wavelength $\lambda_0=1$ μm, waist $w_0=5$ μm, $E_0=1$, and $A_N=(0,1)$.

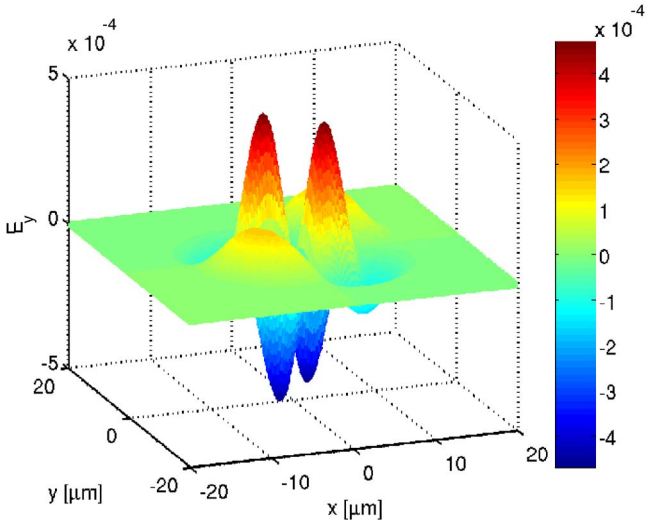

Fig. 12. (Color online) Hollow core angular spectrum solution for E_y in the focal plane ($z=0$) for a wavelength $\lambda_0=1$ μm, waist $w_0=5$ μm, $E_0=1$, and $A_N=(0,1)$.

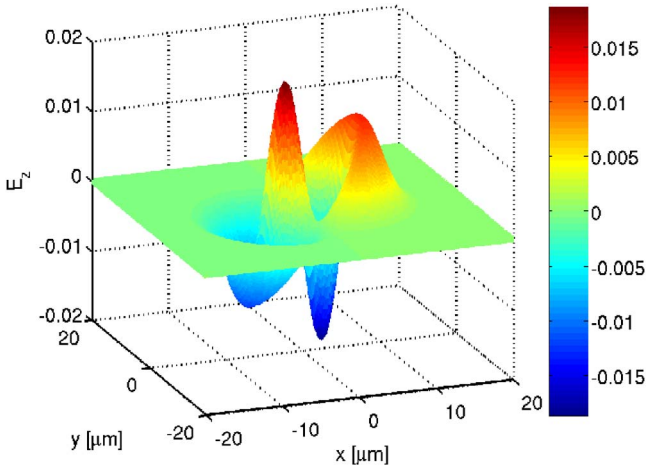

Fig. 13. (Color online) Hollow core angular spectrum solution for E_z in the focal plane ($z=0$) for a wavelength $\lambda_0=1$ μm, waist $w_0=5$ μm, $E_0=1$, and $A_N=(0,1)$.

gradients in the flattened Gaussian and enhanced gradients in the hollow beam—the effect on laser-electron scattering relative to the purely Gaussian case exists for both.

4. COMPARISON BETWEEN THE ANGULAR SPECTRUM AND HERMITE-GAUSSIAN (0,0) MODES

In the high-intensity laser-plasma literature, two focused laser field models are pre-eminent. The most prevalent is the Hermite–Gaussian TEM_{00} mode, which exists as a perturbative expansion in the small diffraction angle $\epsilon = 2/k_0 w_0$. This has been derived several times, for example, by Lax, Louisell, and McKnight,[13] who first introduced longitudinal fields. This was quickly followed up by Davis[14] and then Hora, who reviewed the previous work and solidified the direct connection to laser fields,[10] and later by Barton and Alexander[15] and many others. These solutions impose the final boundary condition that the laser appear as a point spherical wave source in the far field. Wang *et al.* have derived the TEM_{00} more generally allowing for unspecified, alternative boundary conditions.[16] The other prominent formalism is the so-called angular spectrum solution described in the first part of this study.[1] Motivated by the similarities noted in Section 2, the purely Gaussian angular spectrum solution is compared in this section to the TEM_{00} mode and proven to be a formally distinct solution of the wave equation.

A. Hermite–Gaussian (0,0) Laser Mode

The Hermite–Gaussian TEM_{00} mode is generally derived by solving the vector potential wave equation

$$\nabla^2 \mathbf{A} - \frac{1}{c^2}\frac{\partial^2 \mathbf{A}}{\partial t^2} = 0.$$

To accomplish this, the vector potential ansatz

$$\mathbf{A} = \hat{\mathbf{x}} A_0 g(\eta)\Psi(\mathbf{r}) e^{i\eta}$$

is adopted in which A_0 is the magnitude of the lowest-order term, $g(\eta)$ is the temporal envelope function that depends only on the phase $\eta = \omega_0 t - k_0 z$, $\Psi(\mathbf{r})$ is the spatial envelope function, and $e^{i\eta}$ is the plane-wave propagator.[10,13–17] The resulting third-order solution for the three electric field components is shown in Table 1, assuming $g(\eta) \equiv 1$. In the table, Ψ_0 is the familiar lowest-order solution in the series expansion

$$\Psi_0 = \sigma e^{-\sigma\rho^2} = \left(\frac{w_0}{w}\right) e^{-(r^2/w^2)} \exp\left\{ i\left[\eta + \arctan\left(\frac{z}{z_R}\right) - \frac{z r^2}{z_R w^2}\right]\right\},$$

where $\sigma = i z_R/(i z_R + z)$, $z_R = k_0 w_0^2/2$, $w = w_0(1 + z^2/z_R^2)^{1/2}$, $\arctan(z/z_R)$ is the standard Guoy phase shift, and $z r^2/z_R w^2$ is the phase-front curvature. The corresponding third-order magnetic field components are found by simply reversing the roles of x and y.

B. Direct Comparison of the Laser Models

In the limit that $A_0 = 1$ and $A_{N>0} = 0$, the angular spectrum method produces a Gaussian solution similar to the TEM_{00} mode. Both Cicchitelli *et al.* and Quesnel and Mora have asserted that to first order in ϵ, this solution is identical to the TEM_{00} mode.[2,6] This has, in fact, been proven along the laser axis by Borghi *et al.*[18] The question naturally arises whether this integral solution is simply the convergent value of the TEM_{00} series as terms of all orders in ϵ are included, or are these solutions, in fact, distinct?

Table 1. Electric Field Components of the Symmetric TEM_{00} Mode to the Order ϵ^2

$$E_x = E_0 e^{i(\eta - \pi/2)}\Psi_0\left\{1 + \epsilon^2\left[\frac{1}{4}\sigma^2(\rho^2 + 2\bar{x}^2) - \frac{\sigma^3\rho^4}{4}\right]\right\}$$
$$E_y = \frac{1}{2}E_0 e^{i(\eta - \pi/2)}\Psi_0 \epsilon^2 \sigma^2 \bar{x}\bar{y}$$
$$E_z = E_0 e^{i\eta}\Psi_0 \epsilon\bar{x}\left[\sigma + \frac{1}{4}\epsilon^2(3\sigma^2\rho^2 - \sigma^4\rho^4)\right]$$

The magnetic field components are formally identical with only the roles of x and y reversed.

To compare the symmetric solutions and determine whether they can be equated for any boundary condition, and, hence, any choice of the unknown constants introduced by Wang *et al.*,[16] a comparable series expansion in ϵ^2 of the angular spectrum fields is required. To obtain this, note that the functions $(1 - \epsilon^2 t)^{\pm 1/2}$ can be expanded as

$$\sqrt{1 - \epsilon^2 t} = 1 - \frac{1}{2}\sum_{n=1}^{\infty} \frac{\Gamma_{n-1/2}}{n!}\epsilon^{2n} t^n, \tag{6}$$

$$\frac{1}{\sqrt{1 - \epsilon^2 t}} = \sum_{n=0}^{\infty} \frac{\Gamma_{n+1/2}}{n!}\epsilon^{2n} t^n \tag{7}$$

for $t \in [0, \epsilon^{-2})$ and $\Gamma_a \equiv \Gamma(a)/\sqrt{\pi}$. The integral I_1 in the angular spectrum solution of E_x can be directly evaluated to good approximation in the focal plane ($z = 0$) as

$$I_1 = \frac{\epsilon^2}{2}\int_0^{\infty} e^{-t}(1 + \sqrt{1 - \epsilon^2 t}) J_0(2\sqrt{\rho^2 t})\mathrm{d}t \approx \frac{\epsilon^2}{2}\left\{1 - \frac{1}{2}\sum_{n=1}^{\infty}\Gamma_{n-1/2}\epsilon^{2n} L_n\left(\frac{r^2}{w_0^2}\right)\right\} e^{-(r^2/w_0^2)},$$

where the equality holds in the limit of ϵ^2 small, as is naturally required for such an expansion. A similar process can be carried out for the remaining integrals in order to develop a series expansion for $E_x(x, y, z = 0)$, finally yielding

$$E_x = E_0 e^{-(r^2/w_0^2)}\left[1 + \frac{1}{2}\sum_{n=1}^{\infty}\Gamma_{n-1/2}\left(n\frac{y^2}{r^2} - \frac{1}{2}\right)\epsilon^{2n} L_n^0\left(\frac{r^2}{w_0^2}\right) + \frac{1}{4}\epsilon^2\left(\frac{x^2 - y^2}{r^2}\right)\sum_{n=0}^{\infty}\Gamma_{n+1/2}\epsilon^{2n} L_n^1\left(\frac{r^2}{w_0^2}\right)\right],$$

where $L_N^k(x)$ is the Nth order, kth associated Laguerre polynomial.

The purely Gaussian paraxial E_x field is obtained to zeroth order in ϵ from both solution techniques. This validates the conjecture made by both Cicchitelli *et al.* and Quesnel and Mora about the equivalence of the first-order solutions. Both methods also generate higher-order terms

that produce flattened Gaussian contributions to E_x. The series Hermite–Gaussian solution exhibits contributions from both asymmetric solutions. In the angular spectrum solution, however, such terms have arisen solely from the B_y boundary condition.

As an explicit comparison, the order of ϵ^2 term of the angular spectrum E_x is

$$E_x^{(2)}(x,y,z=0)=\frac{E_0}{4}\left(\frac{2x^2-r^2}{w_0^2}\right)e^{-(r^2/w_0^2)}. \tag{8}$$

Appealing to the general boundary condition solution of Wang *et al.*,[16] the TEM_{00} mode, however, gives the second-order field,

$$E_x^{(2)}=\frac{E_0}{4}\left\{-(iC_1+2)\left(\frac{r}{w_0}\right)^4+\left[2\left(\frac{x^2}{w_0^2}\right)+(iC_1+3)\left(\frac{r}{w_0}\right)^2\right]\right\}e^{-(r^2/w_0^2)}, \tag{9}$$

where C_1 is the first constant of integration introduced by Wang *et al.*[16] No value of the constant C_1 can be chosen to equate these two solutions. Thus, the Hermite–Gaussian and angular spectrum methods do, indeed, generate distinct solutions of the Maxwell wave equation to the order of ϵ^2, regardless of the boundary condition used to close the Hermite–Gaussian system. The expression that is valid for a particular laser beam must be determined physically by the specific boundary condition present in the system.

Figure 14 shows the difference between the TEM_{00} solution and the exact angular spectrum solution ($E_x^{\mathrm{TEM}}-E_x$) for E_x in the focal plane for $E_0=1$ and $w_0=5\ \lambda_0$. The constant $C_1=2i$ has been chosen to fit the standard spherical wave boundary condition, as shown in Table 1. This difference has been calculated by numerically evaluating the exact angular spectrum solution and the TEM_{00} mode to fifth order in ϵ. This is illustrated by the dots. This deviation can be calculated directly from Eqs. (8) and (9), yielding

$$\Delta E_x=\frac{1}{4}E_0\epsilon^2\left(\frac{r^2}{w_0^2}\right)\left(2-\frac{r^2}{w_0^2}\right)e^{-(r^2/w_0^2)}, \tag{10}$$

where again $\epsilon=2/k_0w_0$. This is the solid curve of Fig. 14.

This deviation between the field models is, in fact, of the form of a flattened Gaussian: cf. Eq. (1). Therefore, the TEM_{00} mode can be matched to the order of ϵ^4 by choosing $A_0=1$, $A_1=(1/2)\epsilon^2$, and $A_2=-(1/4)\epsilon^4$. Owing to the flattened Gaussian terms generated in $E_x(B_y)$ from the boundary condition specified for $B_y(E_x)$, though, these two solutions can be matched to any order in ϵ^2, but never exactly.

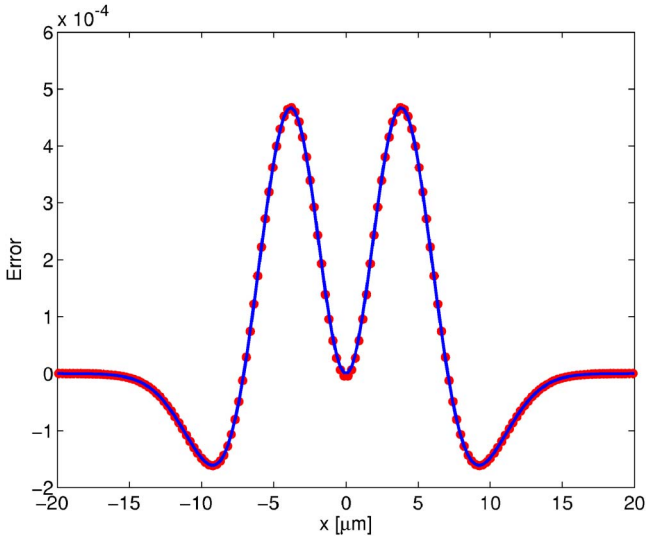

Fig. 14. (Color online) Absolute difference between the symmetric TEM_{00} and angular spectrum solutions for E_x along $y=z=0$ for a wavelength $\lambda_0=1\ \mu$m and waist $w_0=5\ \mu$m corresponding to $\epsilon^2=4.1\times10^{-3}$ and E_0 normalized to 1. The dots have been calculated from the field models and the solid curve is the result predicted by Eq. (10).

5. CONCLUSION

In this study, the six symmetric electromagnetic field components of a focused laser with a general, flattened Gaussian transverse profile have been derived *exactly* in integral form by the use of Fourier transform techniques, also known as the angular spectrum of the plane-wave method. This flattened Gaussian integral solution and the related Gaussian solutions derived previously[2,6,19] are cumbersome and computationally expensive to evaluate on the large scales required when modeling realistic problems. Here, the integrals have been evaluated exactly analytically, fully exploiting the formal symmetry of each integrand for both tight ($w_0\lesssim10\lambda_0$) and loose ($w_0\gtrsim10\lambda_0$) focusing (cf. Section 2).[1]

Under tight focusing, owing to the redundancy of the functions present in the four resulting series, the simplicity of the recurrence relations connecting each order, and the quickly decaying nature of the expansion coefficients and the spherical Bessel functions, this field model offers a significant reduction in computational expense relative to the integral form: $\gtrsim$2 orders of magnitude. The redefinition of the expansion coefficients used in Ref. 20 also significantly reduces the analytical complexity of the resulting field expressions while adding no computational overhead.[20]

These series solutions greatly increase the practicality of calculating flattened and annular Gaussian phenomena for both tight and loose focusing. The flat-top field models outlined in Part I of this study all represent scalar propagation models. The vector series derived here and in Part I (Ref. 1) extend these to include a full vector character for an arbitrary spot size. The formal prototype used also gives the user an infinite set of fitting parameters allowing great flexibility in matching a realistic laser profile, including nonideal Gaussians with flattened profiles, purposefully created flat-top beams, and even annular beams in addition to the standard Gaussian profile. Inclusion of even one or two additional terms generates a wide array of flattened and hollow Gaussian beam profiles, as shown in Section 3.

The loose focusing series derived herein possesses many formal similarities to the standard Hermite–Gaussian (0,0) mode. To investigate the depth of these relations, the Gaussian integral solution and, by extension,

the analytical series solutions of this paper and Part I have been compared to the more ubiquitous Hermite–Gaussian (0,0) mode by analyzing the associated boundary conditions generating each model.[1] In fact, these two forms are found to be distinct solutions exhibiting discrepancies arising at the order of $\epsilon^2=\lambda_0^2/\pi^2w_0^2$. That is, when $w_0 \gtrsim 10\lambda_0$ and terms of the order ϵ^2 can safely be neglected, the TEM_{00} mode and the purely Gaussian perturbative series derived in Eq. (5) are shown to be identical, but when terms of the order of ϵ^2 become appreciable, the models are no longer equal. In fact, the Hermite–Gaussian mode takes on a flattened Gaussian character.

Flattening and nonidealities in a nominally Gaussian laser can become important especially when simulating phenomena strongly dependent upon the longitudinal laser fields, as the spatial profile of the these components depends critically on the shape of the primary field component. Nonparaxial fields have been shown to be of primary importance in modeling direct laser-electron scattering through what is often termed the principle of nonlinearity.[2,4,10,12] Even small corrections to the laser fields can have a significant impact on the electrodynamics of the system. Therefore, any flattening of the laser beam profile tends to alter these anticipated outcomes. Flat-top beams also find use in laser amplifiers where the flattened shape limits self-focusing. The series derived herein allow for easy and flexible modeling of realistic laser profiles under all focusing conditions.

ACKNOWLEDGMENTS

The authors acknowledge support for this work from the National Science Foundation and from the Chemical Sciences, Geosciences, and Biosciences Division of the Office of Basic Energy Sciences, U.S. Department of Energy. S. M. Sepke also thanks Matthew Rever for many helpful and insightful discussions. S. M. Sepke was supported in part by Sandia National Laboratories, Department of Defense-Subcontracts, award 26588.

S. M. Sepke's e-mail address is ssepke2 @unlserve.unl.edu.

REFERENCES

1. S. Sepke and D. Umstadter, "Analytical solutions for the electromagnetic fields of flattened and annular Gaussian laser modes. I. Small *F*-number laser focusing," J. Opt. Soc. Am. B **23**, 2157–2165 (2006).
2. L. Cicchitelli, H. Hora, and R. Postle, "Longitudinal field components for laser beams in vacuum," Phys. Rev. A **41**, 3727–3732 (1990).
3. B. W. Boreham and B. Luther-Davies, "High-energy electron acceleration by ponderomotive forces in tenuous plasmas," J. Appl. Phys. **50**, 2533–2538 (1979).
4. S. Banerjee, S. Sepke, R. Shah, A. Valenzuela, A. Maksimchuk, and D. Umstadter, "Optical deflection and temporal characterization of ultrafast laser-produced electron beams," Phys. Rev. Lett. **95**, 035004 (2005).
5. B. W. Boreham and H. Hora, "Debye length discrimination of nonlinear laser forces acting on electrons in tenuous plasmas," Phys. Rev. Lett. **42**, 776–779 (1979).
6. B. Quesnel and P. Mora, "Theory and simulation of the interaction of ultraintense laser pulses with electrons in vacuum," Phys. Rev. E **58**, 3719–3732 (1998).
7. A. Maltsev and T. Ditmire, "Above threshold ionization and in tightly focused, strongly relativistic laser fields," Phys. Rev. Lett. **90**, 053002 (2003).
8. H. Hora, W. Scheid, T. Hauser, Y. Kato, Y. Kitagawa, K. Mima, and T. Yamanaka, "Free wave laser acceleration of electrons and consequences for the Umstadter experiment," in *Proceedings of the 13th International Conference on Laser Interaction and Related Plasma Phenomena*, AIP Conf. Proc. No. 406 (AIP, 1997), p. 495.
9. S. Masuda, M. Kando, H. Kotaki, and K. Nakajima, "Suppression of electron scattering by the longitudinal components of tightly focused laser fields," Phys. Plasmas **12**, 013102 (2005).
10. H. Hora, *Physics of Laser Driven Plasmas* (Wiley, 1981).
11. H. Hora, M. Hoelss, W. Scheid, J. W. Wang, Y. K. Ho, F. Osman, and R. Castillo, "Acceleration of electrons in vacuum by lasers and the accuracy principle of nonlinearity," in *High-Power Lasers in Energy Engineering*, K. Mima, G. L. Kulcinski, and W. Hogan, eds., Proc. SPIE **3886**, 145–156 (2000).
12. H. Hora, *Laser Plasma Physics* (SPIE, 2000).
13. M. Lax, W. H. Louisell, and W. B. McKnight, "From Maxwell to paraxial wave optics," Phys. Rev. A **11**, 1365–1370 (1975).
14. L. W. Davis, "Theory of electromagnetic beams," Phys. Rev. A **19**, 1177–1179 (1979).
15. J. P. Barton and D. R. Alexander, "Fifth-order corrected electromagnetic field components for a fundamental Gaussian beam," J. Appl. Phys. **66**, 2800–2802 (1989).
16. J. X. Wang, W. Sheid, M. Hoelss, and Y. K. Ho, "Fifth-order corrected field descriptions of the Hermite–Gaussian (0,0) and (0,1) mode laser beam," Phys. Rev. E **64**, 066612 (2001).
17. Y. I. Salamin and C. H. Keitel, "Electron acceleration by a tightly focused laser beam," Phys. Rev. Lett. **88**, 095005 (2002).
18. R. Borghi, A. Ciattoni, and M. Santarisiero, "Exact axial electromagnetic field for vectorial Gaussian and flattened Gaussian boundary distributions," J. Opt. Soc. Am. A **19**, 1207–1211 (2002).
19. P. Varga and P. Török, "The Gaussian wave solution of Maxwell's equations and the validity of scalar wave approximation," Opt. Commun. **152**, 108–118 (1998).
20. S. Sepke and D. Umstadter, "Exact analytical solution for the vector electromagnetic field of Gaussian, flattened Gaussian, and annular Gaussian laser modes," Opt. Lett. **31**, 1447–1449 (2006).